Estimation of Pressure Drop for Vertical Pneumatic Transport of Solids

JENNINGS H. JONES, WALTER G. BRAUN, THOMAS E. DAUBERT, and H. DONALD ALLENDORF

Pennsylvania State University, University Park, Pennsylvania

Many correlations have been proposed for the calculation of the pressure drop in pneumatic solids transfer lines. However, most of them have been for horizontal tubes with only a few applying to vertical tubes. The present work (*1*) was initiated to develop expressions for the estimation of pressure drop for the conveyance of solids of different densities and diameters in vertical tubes with only easily determined physical properties of the solid particles.

The data of many investigators have been summarized by Zenz and Othmer (*15*) and Leva (*10*), who have recommended methods for both horizontal and vertical transport calculations. Most of these researchers correlated their data using the concept that the ratio of the total pressure drop to that of the fluid alone was a linear function of the specific loading (θ). The basic method of Cramp and Priestly (*3*), which consisted of separating the pressure drop into its individual components, has been followed by Hariu and Molstad (*6*) and Uspenskii (*13*). The modified Fanning friction factor approach of Belden and Kassel (*2*) has been utilized by Mehta et al. (*11*) and Gopichand et al. (*5*). Zenz (*14*), Frantz (*4*), and Razumov (*12*) also have recommended methods for the calculation of pressure drop. Korn (*9*) approached the problem by assuming that the total pressure drop is the sum of the pressure drop due to pipe roughness plus the pressure drop that is caused by the suspended material.

THEORY

The pressure drop in the vertical transportation of solid particles can be ascribed to six factors: acceleration of the solid particles, static head of the solid particles, friction between the fluid media and the wall, acceleration of the fluid media, friction between the solid particles and the wall of the retaining pipe, and friction between the solid particles and the fluid media.

The pressure drop due to acceleration of the solid particles can be represented as

$$\Delta p_{as} = \frac{\rho_d u_p^2}{2g} \tag{1}$$

where ρ_d is the dispersed density of the solids.

$$\rho_d = \frac{4 w_p}{3600 \pi D_t^2 u_p} \tag{2}$$

The pressure loss due to static head of the solid particles may be represented by

$$\Delta p_s = \rho_d L_f = \frac{w_p L_f}{900 \pi D_t^2 u_p} \tag{3}$$

The friction caused by the fluid flowing through the pipe can readily be calculated from standard Fanning friction factor equations, while the contribution of the fluid acceleration can be represented by

$$\Delta p_{af} = \frac{\rho_f u_f^2}{2g} = h \tag{4}$$

The final contributions to the pressure drop are the friction between the particles and the wall and the friction between the solid particles and the fluid medium. An approach suggested by Korn (*9*) for evaluating solid-fluid pressure drop assumes that if there are no acceleration losses, the friction caused by the solid particles can be expressed as a single term. The pressure drop of an unladen fluid in a pipe of length L_f is then given by

$$\Delta p = f h \frac{L_f}{D_t} \tag{5}$$

where h is the dynamic pressure of the fluid, Δp_{af}, as given by Equation (4).

Furthermore, the unladen fluid pressure drop Δp^* in a pipe one diameter in length yields

$$\frac{\Delta p^*}{h} = f \tag{6}$$

Assuming that there is a relationship between the specific loading θ and the pressure drop Δp_m^*, caused by the suspended material in a pipe one diameter in length, we see that

$$\frac{\Delta p_m^*}{h} = y \theta^x \tag{7}$$

Thus the total frictional pressure drop per unit diameter of pipe length Δp_f^*, caused by the unladen fluid and the suspended material, is given by the following equations:

$$\Delta p_f^* = \Delta p^* + \Delta p_m^* \cdot \tag{8}$$

$$\frac{\Delta p_f^*}{h} = f + y \theta^x \tag{9}$$

The friction factor for the solids f_s may be considered to be

$$f_s = \frac{\Delta p_f^*}{h} - f = y \theta^x \tag{10}$$

The total pressure drop if acceleration effects are present may then be represented by

$$\Delta p_T = \frac{\rho_d u_p^2}{2g} + \frac{\rho_f u_f^2}{2g} + \rho_d L_f + (f + f_s) h \frac{L_f}{D_t} \tag{11}$$

EXPERIMENTAL PROCEDURE

The apparatus used to determine the pressure drop for pneumatic transport has been described in a previous paper (*8*). Three different steel lift lines of 0.305, 0.402, and 0.870 in. I.D. were used. The lines consisted of two horizontal sections each approximately 3 ft. long and a vertical lift section 21.2 ft. long. Pressure taps were equally spaced at three points along this vertical section.

The data on pressure drop in the lift line were obtained with air used as the carrier gas. Its flow was measured with

H. Donald Allendorf is with Aerochem Research Laboratories, Inc., Princeton, New Jersey.

an orifice meter which had been calibrated with a low-pressure orifice prover. Since the carrier gas was under pressure while lifting the solids, the orifice meter was calibrated at various static pressures. The flow rate of the air (in cubic feet per hour) in the lift line was then determined from the pressure drop across the orifice meter and the static pressure at the top pressure tap.

The solid particles were circulated in the apparatus until steady state was reached, after which the solids and air flow rates in the lift line were determined. The pressure drop values between all pairs of pressure taps were measured by differential manometers with water or mercury used as the manometric liquid, depending on the magnitude of the pressure drop. Preliminary experiments showed that pressure drops between equally spaced pairs of pressure taps along the transport line were equal. Thus only an overall pressure drop needed to be recorded and pressure drop due to acceleration of the solid particles over the region of interest could be neglected.

Pressure drop values were determined for twelve different solid particles of varying diameters (200 to 765 microns) densities (156 to 475 lb./cu. ft.), and surface shape factors (0.40 to 0.95). Seven hundred and fifty-three measurements were made at numerous solid and air flow rates.*

The source of materials as well as the procedures used for determining the properties of the solid particles and the method of determining the rate of solids flowing in the apparatus were reported (*8*).

DISCUSSION

To visualize qualitatively the behavior of the pneumatic system for cocurrent fluid-solid upflow, the data for each solid in each tube size were plotted on a fluid-solid flow diagram as described by Zenz and Othmer (*15*). The data were all located in the region of fully dispersed flow. The superficial fluid velocity for nearly all of the experimental series decreased from a high value to a value approaching the choking velocity. Figure 1 shows a representative plot of these data for one particle size, particle density, and three tubing sizes.

Several attempts were made to correlate the pressure drop data. The method of Belden and Kassel (*2*) yielded average deviations of about 15% and was rejected. The correlation finally selected was a modification of the method of Korn which consisted of plotting on logarithmic paper the solids friction factor (f_s) against the specific loading θ. An example of this type plot for fused alumina No. 36 is shown in Figure 2. The twelve plots of the logarithm of the solids friction factor vs. the logarithm of the specific loading yielded essentially straight lines which could be represented by Equation (10).

Although in Figure 2 it appears that the ratio of the particle diameter to the tube diameter may also be a correlating parameter, this was found not to be the case when all twelve plots were analyzed for this effect. These data, thus, further confirm the results of Korn (*9*) and Belden and Kassel (*2*) that pressure drop is nearly independent of the diameter ratio.

When the plots were analyzed for the values of x and y in Equation (10), it was found that when the surface areas of the solid particles were less than about 6,300 sq.ft./cu.ft., the value of the exponent x was approximately equal to unity. When the area exceeded 6,300 sq.ft./cu.ft., x was less than 1. The three air-solid systems which had values of x below unity were correlated by

$$x\ (A_o > 6{,}300) = \left(\frac{6{,}300}{A_o}\right)^{1/3} \qquad (12)$$

Since the surface area of the solid particles is some inverse function of the terminal velocity, it is also a function of the terminal velocity head h_t. A large surface area represents a small terminal velocity. As the surface area decreases, the terminal velocity increases and h/h_t approaches unity. Korn showed that as h/h_t approached unity so did the exponent x and as the velocity head ratio increased above unity the exponent x decreased until at values approaching infinity the exponent again approached unity. Thus Equation (12) is not valid for determining x near h/h_t values of infinity. Since the upper limit of the surface area has not been determined, the equation can only be used with confidence within the range of this investigation (6,300 to 20,000 sq.ft./cu.ft.).

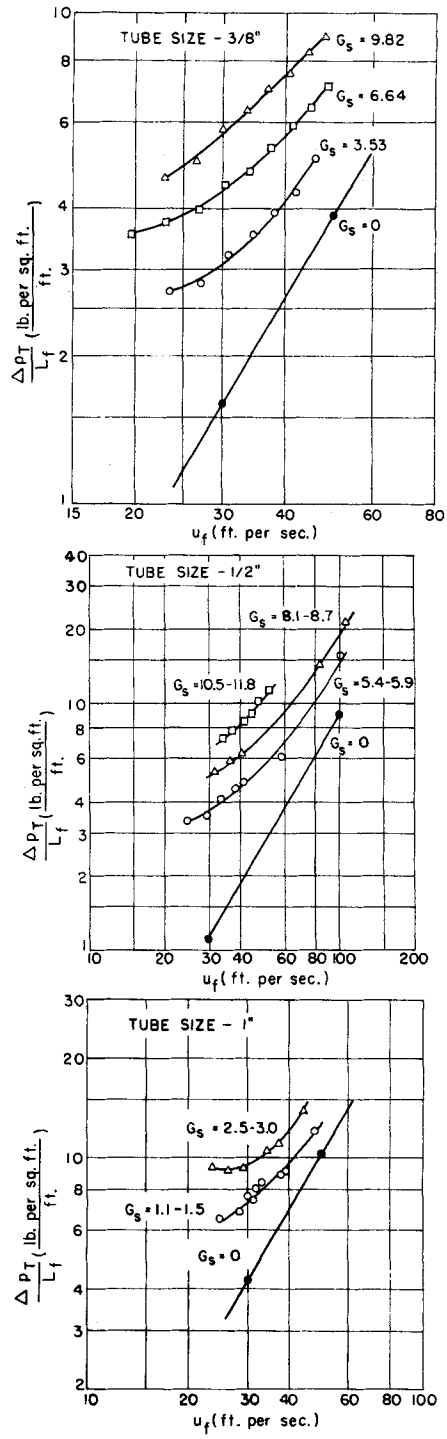

Fig. 1. Fluid-solid flow diagrams. Fused alumina No. 36; D_p = 740 μ, ρ_s = 243 lb./cu.ft.

Complete data have been deposited as document 9358 with the American Documentation Institute, Photoduplication Service, Library of Congress, Washington 25, D. C., and may be obtained for $5.00 for photoprints or $2.25 for 35-mm. microfilm.

The values of y in Equation (10) increased with increasing surface area of the solid particles and decreased with increasing surface shape factor. By the use of trial and error procedures and these two solid properties, the values of y were correlated by

$$y = 1.89 \times 10^{-6} \frac{A_o}{\chi^{1/2}} \qquad (13)$$

The values of both x and y obtained experimentally are compared with those calculated from Equations (12) and (13) in Table 1.

When Equation (13) is substituted in Equation (10), the following relationship is obtained

$$\frac{\Delta p_f^*}{h} - f = f_s = 1.89 \times 10^{-6} \frac{A_o}{\chi^{1/2}} \theta^x \qquad (14)$$

When Equation (14) was used to calculate the solids friction factor at a specific loading θ of ten (a value rarely exceeded in pneumatic conveyance), it was noted that with one exception the calculated value differed by a maximum of 23% from the experimental value obtained. For the case of the single exception, steel shot C_1, the deviation from the experimental value was 45%. However, when the pressure drop values due to the air and static pressure were added, the error was greatly reduced and the deviation was less than 13% except for steel shot C_1, which deviated by 25%. When a specific loading of one was used, the deviation from the experimental value with Equation (14) was in the majority of cases less than 5% with a maximum deviation of 11%.

Using an IBM 7074 digital computer, we calculated total pressure drop values using this approach and the approach of Hinkle (7) as reported by Zenz and Othmer (15). Only the Hinkle method was used for comparison, as no other method available was sufficiently general so that the necessary parameters could be estimated for its use. Each of the data points was checked against the experimental values. The average deviation from the experimental values based on all 753 data points was 23.1% with Hinkle's correlation and 14.0% with the correlation of this work. The corresponding average bias deviations were −17.8 and +3.9%, respectively.

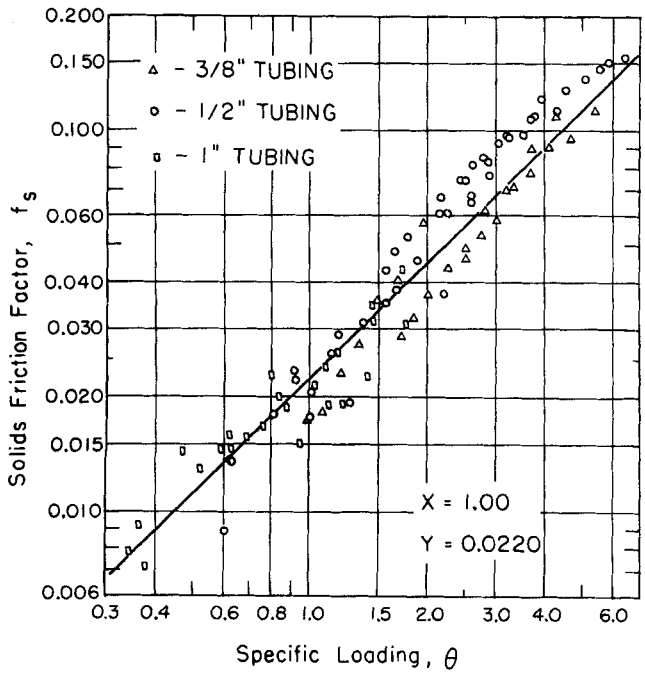

Fig. 2. Effect of specific loading on the solids friction factor for the system of fused alumina No. 36 and air.

TABLE 1. VALUES OF x AND y IN EQUATION (10) FOR VARIOUS AIR-SOLID SYSTEMS

Air temperature = 24°C.

Solid used in air-solid system	Experimental values		Calculated values*	
	x	y	x	y
Glass beads No. 109	1.00	0.0110	1.00	0.0107
Glass beads No. 106	1.00	0.0088	1.00	0.0072
Fused alumina No. 100	0.71	0.0520	0.68	0.0570
Fused alumina No. 60	0.89	0.0340	0.88	0.0272
Fused alumina No. 36	1.00	0.0220	1.00	0.0182
Zircon silica No. 1	0.99	0.0094	1.00	0.0091
Zircon silica No. 2	1.00	0.0110	1.00	0.0135
Steel shot A	0.98	0.0093	1.00	0.0101
Steel shot C_1	0.92	0.0100	0.97	0.0134
Steel shot C_2	1.00	0.0105	1.00	0.0126
Steel shot D_1	1.00	0.0066	1.00	0.0070
Steel shot D_2	0.98	0.0081	1.00	0.0076

* Values were calculated from Equations (12) and (13).

USE OF THE METHOD

Fluid rate and density, tubing diameter, and solids rate, density, surface area, and surface shape factor are the only quantities which need be known for the use of this method. The total pressure drop can be calculated from Equation (11). Friction factors for air can be obtained from standard Fanning type charts, while solids friction factors can be obtained from Equation (14).

Attempts were made to apply this method to literature values of pressure drop in pneumatic conveyance. However, in many cases it was found to be extremely difficult to determine the necessary physical properties of the solid materials and whether acceleration effects were present. More complete data are necessary before a definitely valid comparison can be made.

NOTATION

A_o = surface area of solid particles, sq.ft./cu.ft.
D_p = statistical diameter of particle based on specific surface per unit volume, ft.
D_t = diameter of pipe or tubing, ft.
f = friction factor for air, dimensionless
f_s = friction factor for solids, dimensionless
g = local gravitational constant, ft./sec.^{2}
G_s = mass flow rate of solids, lb./(sec.)(sq.ft.)
h = velocity head of fluid, lb./sq.ft. [as given by Equation (4)]
h_t = terminal velocity head, lb./sq.ft.
L_f = length of lift line, ft.
Δp = pressure drop of unladen fluid, lb./sq.ft.
Δp^* = pressure drop of unladen fluid per one diameter pipe length, lb./sq.ft.
Δp_{as} = pressure drop due to acceleration of the solids lb./sq.ft.
Δp_{af} = pressure drop due to acceleration of the fluid, lb./sq.ft.
Δp_f^* = total pressure drop due to friction only per one diameter pipe length, lb./sq.ft.
Δp_m^* = pressure drop due to particulate material per one diameter pipe length, lb./sq.ft.
Δp_s = pressure drop due to static head, lb./sq.ft.
Δp_T = total pressure drop, lb./sq.ft.
u_f = velocity of fluid media, ft./sec.
u_p = velocity of solid particles, ft./sec.
w_p = solids rate, lb./hr.
x = exponent, dimensionless

y = coefficient, dimensionless
θ = specific loading, lb. solids/lb. fluid
ρ_d = dispersed density of solids, lb./cu.ft. [as given by Equation (2)]
ρ_f = density of fluid media, lb./cu.ft.
χ = surface shape factor of solid particles, dimensionless

LITERATURE CITED

1. Allendorf, H. D., M.S. thesis, Pennsylvania State Univ., University Park (1960).
2. Belden, D. H., and L. S. Kassel, *Ind. Eng. Chem.*, **41**, 1174 (1949).
3. Cramp, W., and A. Priestly, *Engineer*, **137**, 89 (1924).
4. Frantz, J. F., *Chem. Eng.*, **69**, No. 19, 161; No. 20, 89; No. 22, 103 (1962).
5. Gopichand, T., K. J. R. Sarma, and M. N. Rao, *Ind. Eng. Chem.*, **51**, 1449 (1959).
6. Hariu, O. H., and M. L. Molstad, *ibid.*, **41**, 1148 (1949).
7. Hinkle, B. L., Ph.D. thesis, Georgia Inst. Technol. (1953).
8. Jones, J. H., W. G. Braun, T. E. Daubert, and H. D. Allendorf, *A.I.Ch.E. J.*, **12**, 1070 (1966).
9. Korn, A. H., *Chem. Eng.*, **57**, No. 3, 108 (1950).
10. Leva, Max, "Fluidization," McGraw-Hill, New York (1959).
11. Mehta, N. C., J. M. Smith, and E. W. Comings, *Ind. Eng. Chem.*, **49**, 986 (1957).
12. Razumov, I. M., *Intern. Chem. Eng.*, **2**, No. 4, 539 (1962).
13. Uspenskii, V. A., *Ekon. Topliva Za.*, **8**, No. 3, 26 (1951).
14. Zenz, F. A., *Petrol. Refiner*, **36**, No. 4, 173; No. 5, 261; No. 6, 133; No. 7, 175; No. 8, 147; No. 9, 305; No. 10, 162; No. 11, 321 (1957).
15. Zenz, F. A., and D. F. Othmer, "Fluidization and Fluid Particle Systems," Reinhold, New York (1960).

The Use of Residual Analysis for Building Mechanistic Models

WILLIAM J. HILL

Allied Chemical Corporation, Buffalo, New York

REIJI MEZAKI

Yale University, New Haven, Connecticut

The use of residuals of a diagnostic parameter for kinetic modeling was developed and demonstrated in two previous papers (*1*, *2*). In the second paper (*2*) the importance of the selection of an initial model was emphasized for the successful use of the proposed technique. The aims of this communication are threefold. First, by means of mathematical statistics, we wish to prove the existence of definite correlation between the residuals associated with an inadequate model and the concentration level of an improperly described component. Second, we wish to illustrate that an appropriate choice of an experimental design can simplify the analysis. Third, we will illustrate a situation where a residual analysis may be misleading when not interpreted properly.

RESIDUALS AND CONCENTRATION LEVELS

In the earlier papers, Hougen-Watson reaction models were postulated for the complete catalytic oxidation of methane and the following model was found to be appropriate: gaseous methane and adsorbed oxygen react and produce both adsorbed carbon dioxide and adsorbed water. In the true case, the value of the diagnostic parameter C_1 can be given by

$$C_1 = b_o + b_2 x_2 + b_3 x_3 + b_4 x_4 + \epsilon \qquad (1)$$

Suppose instead we consider, as an initial trial model, a model for which the value of the calculated diagnostic parameter is

$$\hat{C}_1 = \hat{b}_o + \hat{b}_2 x_2 + \hat{b}_4 x_4 \qquad (2)$$

Note that this model implies that gaseous methane reacts with adsorbed oxygen, producing nonadsorbed carbon dioxide and adsorbed water.

Now Equation (1) may be simplified to the matrix form

$$\mathbf{C}_1 = \mathbf{X}_1 \underline{\theta}_1 + \mathbf{X}_3 \underline{\theta}_3 + \underline{\epsilon} \qquad (3)$$

where

$$\mathbf{X}_1 = [\mathbf{1},\ \mathbf{x}_2,\ \mathbf{x}_4]$$
$$\mathbf{X}_3 = [\mathbf{x}_3]$$
$$\underline{\theta}_1 = \begin{bmatrix} b_o \\ b_2 \\ b_4 \end{bmatrix}$$
$$\underline{\theta}_3 = [b_3]$$

$\mathbf{C}_1$ is the $n \times 1$ vector of the diagnostic parameters (n is the number of observations), $\mathbf{X}_1$ is an $n \times 3$ matrix, and $\mathbf{X}_3$ is an $n \times 1$ vector. $\underline{\theta}_1$ and $\underline{\theta}_3$ are 3×1 and 1×1 vectors, respectively.

Similarly, Equation (2) in vector form is

$$\hat{\mathbf{C}}_1 = \mathbf{X}_1 \hat{\underline{\theta}}_1 \qquad (4)$$

where

$$\hat{\underline{\theta}}_1 = \begin{bmatrix} \hat{b}_o \\ \hat{b}_2 \\ \hat{b}_4 \end{bmatrix}$$